

## T2 relaxation time is related to liver fibrosis severity

Alexander R. Guimaraes<sup>1,2,3</sup>, Luiz Siqueira<sup>1</sup>, Ritika Uppal<sup>2</sup>, Jamu Alford<sup>2</sup>, Bryan C. Fuchs<sup>4</sup>, Suguru Yamada<sup>4</sup>, Kenneth Tanabe<sup>4</sup>, Raymond T. Chung<sup>5</sup>, Gregory Lauwers<sup>6</sup>, Michael L. Chew<sup>1</sup>, Giles W. Boland<sup>1</sup>, Duhyant V. Sahani<sup>1</sup>, Mark Vangel<sup>7</sup>, Peter F. Hahn<sup>1</sup>, Peter Caravan<sup>2</sup>

<sup>1</sup>Division of Abdominal Imaging and Interventional Radiology, Department of Radiology, Massachusetts General Hospital, Boston, MA 02114, USA;

<sup>2</sup>Martinos Center for Biomedical Imaging, Department of Radiology, Massachusetts General Hospital, Charlestown, MA 02129, USA; <sup>3</sup>Section for Body Imaging, Department of Radiology, Oregon Health & Sciences University, Portland, OR 97239, USA; <sup>4</sup>Division of Surgical Oncology, Department of Surgery, <sup>5</sup>Division of Hepatology, Department of Medicine, <sup>6</sup>Department of Pathology, <sup>7</sup>Department of Biostatistics, Massachusetts General Hospital, Boston, MA 02114, USA

Correspondence to: Alexander R. Guimaraes, MD, PhD. Department of Radiology, Oregon Health & Sciences University, Portland, OR 97239, USA. Email: guimaraa@ohsu.edu.

**Background:** The grading of liver fibrosis relies on liver biopsy. Imaging techniques, including elastography and relaxometric, techniques have had varying success in diagnosing moderate fibrosis. The goal of this study was to determine if there is a relationship between the T2-relaxation time of hepatic parenchyma and the histologic grade of liver fibrosis in patients with hepatitis C undergoing both routine, liver MRI and liver biopsy, and to validate our methodology with phantoms and in a rat model of liver fibrosis.

**Methods:** This study is composed of three parts: (I) 123 patients who underwent both routine, clinical liver MRI and biopsy within a 6-month period, between July 1999 and January 2010 were enrolled in a retrospective study. MR imaging was performed at 1.5 T using dual-echo turbo-spin echo equivalent pulse sequence. T2 relaxation time of liver parenchyma in patients was calculated by mono-exponential fit of a region of interest (ROI) within the right lobe correlating to histopathologic grading (Ishak 0–6) and routine serum liver inflammation [aspartate aminotransferase (AST) and alanine aminotransferase (ALT)]. Statistical comparison was performed using ordinary logistic and ordinal logistic regression and ANOVA comparing T2 to Ishak fibrosis without and using AST and ALT as covariates; (II) a phantom was prepared using serial dilutions of dextran coated magnetic iron oxide nanoparticles. T2 weighed imaging was performed by comparing a dual echo fast spin echo sequence to a Carr-Purcell-Meigboom-Gill (CPMG) multi-echo sequence at 1.5 T. Statistical comparison was performed using a paired *t*-test; (III) male Wistar rats receiving weekly intraperitoneal injections of phosphate buffer solution (PBS) control (n=4 rats); diethylnitrosamine (DEN) for either 5 (n=5 rats) or 8 weeks (n=4 rats) were MR imaged on a Bruker Pharmascan 4.7 T magnet with a home-built bird-cage coil. T2 was quantified by using a mono-exponential fitting algorithm on multi-slice multi echo T2 weighted data. Statistical comparison was performed using ANOVA.

**Results:** (I) Histopathologic evaluation of both rat and human livers demonstrated no evidence of steatosis or hemochromatosis. There was a monotonic increase in mean T2 value with increasing degree of fibrosis (control 65.4±2.9 ms, n=6 patients); mild (Ishak 1–2) 66.7±1.9 ms (n=30); moderate (Ishak 3–4) 71.6±1.7 ms (n=26); severe (Ishak 5–6) 72.4±1.4 ms (n=61); with relatively low standard error (~2.9 ms). There was a statistically significant difference between degrees of mild (Ishak <4) *vs.* moderate to severe fibrosis (Ishak >4) (P=0.03) based on logistic regression of T2 and Ishak, which became insignificant (P=0.07) when using inflammatory markers as covariates. Expanding on this model using ordinal logistic regression, there was significance amongst all 4 groups comparing T2 to Ishak (P=0.01), with significance using inflammation as a covariate (P=0.03) and approaching statistical significance amongst all groups by ANOVA (P=0.07); (II) there was a monotonic increase in T2 and statistical significance (ANOVA P<0.0001) between each rat subgroup [phosphate buffer solution (PBS) 25.2±0.8, DEN 5-week (31.1±1.5), and DEN 9-week (49.4±0.4) ms];

(III) the phantoms that had T2 values within the relevant range for the human liver (e.g., 20–100 ms), demonstrated no statistical difference between two point fits on turbo spin echo (TSE) data and multi-echo CPMG data ( $P=0.9$ ).

**Conclusions:** The finding of increased T2 with liver fibrosis may relate to inflammation that may be an alternative or adjunct to other noninvasive MR imaging based approaches for assessing liver fibrosis.

**Keywords:** MRI; liver fibrosis; quantitative imaging; T2 relaxation time; fibrosis imaging biomarkers

Submitted Nov 19, 2015. Accepted for publication Jan 20, 2016.

doi: 10.21037/qims.2016.03.02

View this article at: <http://dx.doi.org/10.21037/qims.2016.03.02>

## Introduction

Chronic liver disease is an important cause of morbidity and mortality throughout the world. Recent studies suggest that there will be approximately 150,000 patients with chronic liver disease diagnosed each year (1,2). Of these 150,000, almost 20%, or an estimated 30,000 patients per year, will have cirrhosis at the time of presentation (1,3). Cirrhosis remains a major public health problem and disease-related complications were associated with nearly 40,000 deaths and more than 1.4 billion dollars spent on medical services in the US (1,3). There is a great need to develop and identify methods of risk stratification and prognosis for patients with chronic liver disease (4,5).

Hepatic fibrosis is the final common pathway for patients with chronic liver disease. The diagnosis and quantification of fibrosis relies on liver biopsy (6), as liver biopsy is currently the standard of reference for detecting and staging hepatic fibrosis (7). However, liver biopsy is an invasive procedure with significant risks, including hemorrhage, infection and visceral perforation (5-7). Moreover, liver biopsy is a poor gold standard, limited by both geographic sampling error within the liver and by inter-observer variation in interpretation of histology with sampling errors in 25–45% cases (5-7).

Noninvasive tests have been applied with varying success to diagnose and stage patients with liver fibrosis (8). Serum markers such as the aspartate aminotransferase (AST) to platelet ratio index (APRI) (9) or composites, serum analyses such as FibroTest<sup>®</sup> or FibroSure<sup>®</sup> can potentially differentiate between those patients with and without significant fibrosis or cirrhosis with sensitivity of 76–81% (6,10). Imaging techniques, which have exploited the increased stiffness exhibited by fibrotic and cirrhotic livers, include ultrasound elastography [transient elastography (TE)] (11-14) and magnetic resonance elastography (MRE)

have had varying success to diagnose moderate fibrosis found pooled estimates for sensitivity and specificity of 70% and 84% respectively (11-13,15-18). The application of diffusion-weighted magnetic resonance imaging (DWI), to patients with liver fibrosis, has demonstrated lower apparent diffusion coefficient (ADC) values in patients with varying degrees of fibrosis as compared to normal controls (7,19). In addition, other MR based imaging biomarkers including T1 and T1rho have demonstrated promise in differentiating varying degrees of liver fibrosis (20-23) with T2 relaxometry demonstrating high variability (20,24,25).

Given the diversity in imaging biomarkers associated with liver fibrosis, we chose to focus on an observation that has been noted in early publications of MRI and the liver: the increased, and heterogeneous signal intensity in fibrotic and cirrhotic MRI examinations of the liver (26,27). Although recent results in the pediatric community do not demonstrate a quantitative relationship between T2 and liver fibrosis stage (24), other results in animal models of liver fibrosis and in humans with chronic liver disease, suggest that the T2 value can separate varying degrees of liver fibrosis in murine models of liver fibrosis (20,25,28,29). Although the etiology of this finding is unknown, it may be related to an increased inflammatory component that has been demonstrated in chronic hepatitis (30) and steatohepatitis (31). Because of increasing interest in quantitative imaging biomarkers associated with disease processes, we investigated retrospectively whether there is a quantitative relationship and correlation between the absolute value of T2 and stage of liver fibrosis. We chose to study this retrospectively from patients with either hepatitis C, all of whom had undergone random non-focal liver biopsy for fibrosis staging and had obtained a clinical MRI within 6 months of their liver biopsy.

As a result of the potential limitations in quantifying the

T2 in routine clinical MRI examinations all performed with a dual echo turbo spin echo (TSE) equivalent sequence, it was important to better understand and study whether any limitations existed with quantification of T2 with this number of echoes. We therefore prepared a phantom containing serial dilutions of ultrasmall superparamagnetic iron oxide magnetic nanoparticles (MNP) and compared the methodologies used in the clinical retrospective study, to more robust, established routines for quantifying T2 [e.g., Carr-Purcell-Meigboom-Gill (CPMG) pulse sequences].

We then applied our methods in a diethylnitrosamine (DEN) rat model of liver fibrosis to test the hypothesis that T2 is a robust quantitative imaging biomarker of liver fibrosis. As no liver model truly mimics the disease seen in humans, we chose a DEN model of liver fibrosis, because of its development of fibrosis and eventual cirrhosis similar to humans (32,33). This sequential progression is not found in many models and rats have a higher propensity for cirrhosis (34). There is also a suggestion that the molecular alterations seen in human cirrhosis are similarly observed in DEN rats and less so in mouse models (35).

## Materials and methods

This study is composed of three parts: (I) a human retrospective study in patients with hepatitis C who had both MRI and liver biopsy comparing T2 relaxation (as determined by a 2 point fit of dual echo turbospin echo T2 data) as obtained by MRI with histological assessment of liver fibrosis and correlative serum assays of liver inflammation [AST and alanine aminotransferase (ALT)]; (II) a phantom study using varying concentrations of iron oxide nanoparticles in order to vary T2 and compare a mono-exponential fit of 2 TE values *vs.* multiple TE values (2–16 TE's); and (III) a study comparing T2 to histologic assays of fibrosis in a rat model of liver fibrosis.

### Clinical study

Approval for this retrospective study was obtained from the hospital ethics committee on human studies. This study is a Health Insurance Portability and Accountability Act (HIPAA) compliant study and patient informed consent was waived.

A search that combined our home-built database of interventional procedures (36,37) with our institution's radiology information database (General Electric Medical

Systems, Milwaukee, WI, USA) sought records of all patients with chronic active hepatitis C in whom a random liver biopsy was performed during the period 07/1999–1/2010, and correlated with all patients undergoing MRI examination of the liver within a time period of 6 months. Patients with iron storage disease (e.g., hemochromatosis), or patients that demonstrated evidence of steatosis on random liver biopsy, or dual phase gradient echo imaging were excluded. The patient population was therefore a homogeneous cohort of patients with hepatitis C derived chronic liver disease. AST, ALT within 30 days of the MRI were collected. Liver biopsy specimens were scored using the Ishak classification system (0–6) and grouped into normal (score 0, n=6), mild (score 1–2, n=30), moderate (score 3–4, n=26), severe (score 5–6, n=61). Patients that demonstrated no evidence of fibrosis pathologically, and no active inflammation based on serologic data were considered control patients.

MR imaging was performed with a phased array body coil (8 channel) on either Siemens 1.5 T Avanto/Allegra (Siemens Medical, Erlangen, GE, Germany) or GE Excite (General Electric Medical Systems, Milwaukee, WI) and included respiratory gated, multi-slice TSE equivalent pulse sequences with dual TE values (46–99 and 84–177 ms) and TR 2,000–3,500 ms, which utilized fat suppression. Field of view (FOV) was 30–40 cm, with matrix 192×144 size 192×144, and number of excitations (NEX) of 2. T1 weighted images were performed following T2 weighted acquisitions [volumetric 3D gradient echo images LAVA (GE), VIBE (Siemens)] prior to and following the administration of 0.1 mmol/kg Gd-DTPA (Magnevist<sup>®</sup>, Bayer Pharmaceuticals, Wayne, NJ, USA).

T2 relaxation time of liver parenchyma in patients was calculated by an abdominal radiologist with greater than 5 years of experience in abdominal MRI, region of interest (ROI) was drawn on the right lobe of the liver (segment 5) on T1 weighted post contrast images in a region that avoided vascular averaging and also ensured liver in adjacent slices, so as to avoid partial volume contamination, and translating them onto the first echo of the dual echo images (so as to avoid bias in areas that may have T2 hyperintensity). T2 relaxation time was performed by a separate radiologist, so as to avoid statistical bias, by using a two-point fit.

The association of liver fibrosis with T2 relaxometry measures was assessed using one way ANOVA, and by using ordinary and ordinal logistic regression, with and without serum biomarkers (AST and ALT) as covariates. Regression

models were compared using the Akaike Information Criterion (AIC), with smaller values indicating preferable models. The statistical significance of T2, both alone, and after adjusting for serum biomarkers, was determined using the likelihood-ratio Chi-square statistics. Computations were done using the R statistics language (38) and specifically the ordinal logistic function 'plot.' (39).

In order to assess whether there was any relationship between T2 relaxometry and liver function tests (AST and ALT), linear regression was performed.

### *Phantom study*

In order to validate the methods of a dual-echo T2 relaxometry measures, we performed a phantom study comparing T2 calculated from mono-exponential fits of CPMG type sequences as compared to double echo TSE in an iron oxide nanoparticle phantom with serial dilutions of saline that contained T2 measures within the breadth normally found in the human abdomen. Our phantoms consisted of one cc of dextran coated magnetic iron oxide nanoparticle (MION 48) ( $R^2=49 \text{ s}^{-1}$ ) (1 mg Fe/mL) diluted with the following fractionations (1:50, 1:100, 1:250, 1:500, 1:1,000, 1:10,000, normal saline) and placed in 50 mL Eppendorf (Fischer Scientific) tubes.

MRI was performed in a single experiment in a 1.5-T Siemens Avanto with TIM technology using a multi-channel array head coil (4 channels). All imaging was performed immediately following phantom production in order to minimize settling, with an asymmetric field of view (FOV) (16×14 cm) and 512×409 matrix using a 4-mm slice thickness, interleaved with no gap, and utilizing fat suppression in order to maintain imaging parameters as close to the human experiment as possible. The CPMG sequences were performed all with TR 5,000 ms and TE (22 ms in 22 ms intervals). The TSE sequences were performed with effective TE of 22 and 86 ms, with an echo train length of 7 and a TR of 5,000. T2 was fit using a mono-exponential fit from measures obtained within a ROI that encompassed the entirety of each tube in the axial plane taking care to avoid partial volume artifacts from adjacent slices with a customized plug-in for Macintosh based DICOM viewer and image analysis platform (Osirix®). Statistical analyses compared T2 for each phantom using a student's paired *t*-test (GraphPad Prism 4, Palo Alto, CA, USA).

### *Animal model*

This study was approved by and all animals were maintained

in accordance with the institutional guidelines of the Massachusetts General Hospital (MGH) Subcommittee on Research Animal Care (SRAC). All animals received humane care according to the criteria outlined in the "Guide for the Care and Use of Laboratory Animals" of the National Academy of Sciences (40). Male Wistar rats received weekly IP injections of DEN at 100 mg/kg or vehicle control (PBS) for either 5 or 8 weeks. Rats were imaged at 6 and 9 weeks after a 1-week washout period to eliminate acute inflammatory effects of DEN. After imaging, the animals were sacrificed and the liver was removed. The liver was then sectioned and fixed in phosphate-buffered 10% formalin for histological analysis by H&E and Masson's trichrome staining.

### *Animal magnetic resonance imaging*

MRI was performed at 4.7 T on a Bruker imaging system (Pharmascan, Karlsruhe, Germany). Animals were placed in a specially constructed cradle and imaged with a home-made bird-cage coil. Animals were anesthetized during imaging with 1–1.5% inhaled isoflurane, and monitored during imaging with respiratory monitoring. Imaging protocols included a Tri-plane and axial TSE localizer. Multi-slice multiecho (MSME) T2-weighted imaging was performed for T2 quantification. The following parameters were utilized: Flip angle =90°; Matrix size (128×64); TR =2,500 ms; TE =16 equally spaced echoes at an interval of 8.6 ms ranging from 8.6 to 137.6 ms; FOV =4.24×2.12 cm; slice thickness =1 mm. T1 weighted imaging was performed (TE =8 ms, TR =217 ms) following the administration of 10 mmol/kg Gd-DTPA. A 1-mL round ROI's were placed by an experienced radiologist with greater than 5 years training in body imaging, within an area of the right lobe of the liver on T1 weighted images (so as to avoid T2 bias) that avoided vascular contamination and also ensured liver in adjacent slices, so as to avoid partial volume contamination, and then copied onto T2 weighed images for T2 quantification. T2 was quantified by using a mono-exponential fitting algorithm for the multi-TE data (Osirix®). T2 was then quantified in all groups and included the following: (I) n=4 PBS normal control rats; (II) n=5 DEN rats treated for 5 weeks, corresponding to moderate (Ishak stage 4) fibrosis; and (III) n=4 DEN rats treated for 8 weeks, which corresponded histologically to Ishak stage 6 cirrhosis. Our fitting algorithm ensured that we minimized echoes below a threshold of 2× the noise floor. The association of liver fibrosis with T2 relaxometry measures was assessed using one way ANOVA.

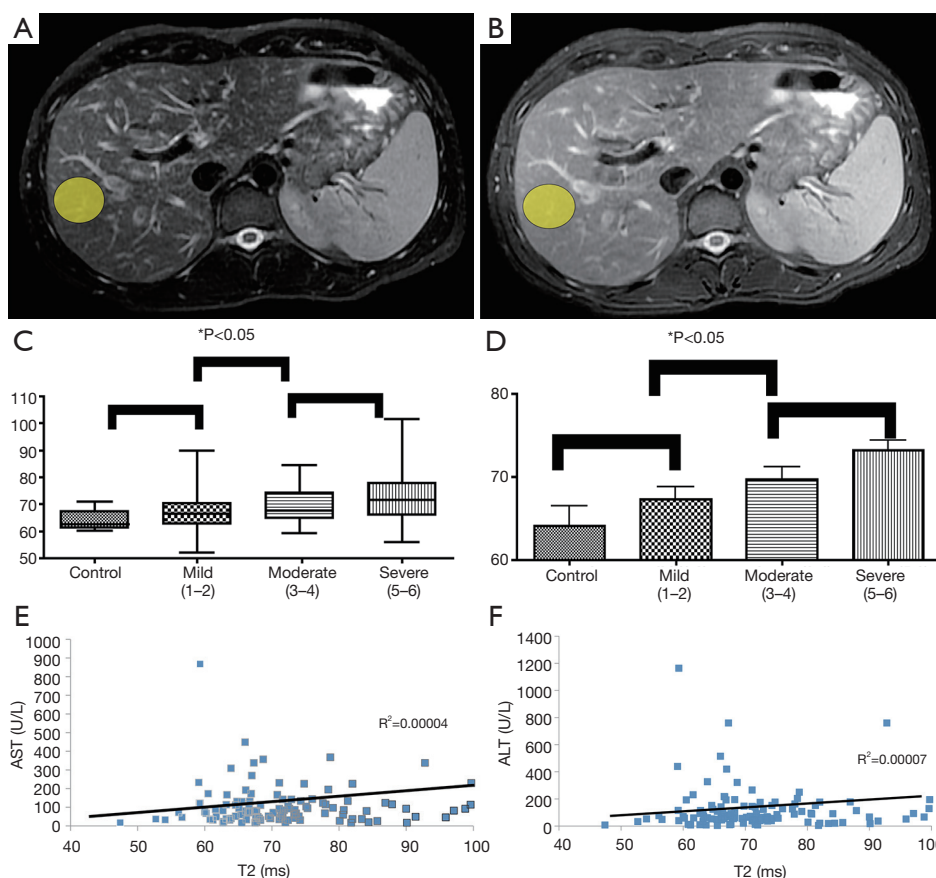


**Figure 1** T2 measures in human liver. (A,B) Examples of ROI's (yellow ellipse) from T2 weighted MRI (TE =60,120; TR =2,000) within the right lobe of the liver avoiding major vessels avoiding areas suffering from phase encoding artifact. (C) Box and whisker plots and column vertical bar graphs (D) of the absolute T2 measurements (control 65.4±2.9 ms; mild (Ishak 1–2) 66.7±1.9 ms; moderate (Ishak 3–4) 71.6±1.7 ms; severe (Ishak 5–6) 72.4±1.4 ms), which demonstrated low standard error (~2.9 ms). Furthermore, there was a monotonically increasing mean T2 value with increasing degree of histologic fibrosis. There was a statistically significant difference between degrees of mild *vs.* severe fibrosis (P=0.03). (E,F) Linear regression analysis comparing AST (E) ( $R^2=0.00004$ ) and ALT (F) ( $R^2=0.00007$ ) to T2 demonstrated no evidence of correlation between these serum markers of inflammation and the T2 biomarker. \*, based on logistic regression and statistical significance amongst all groups by ordinal logistic regression (P=0.01) and ANOVA (P<0.1). ROI, region of interest; AST, aspartate aminotransferase; ALT, alanine aminotransferase.

## Results

### Patient results

Our database query revealed 123 eligible patients. The average time between MRI and biopsy was -8 days with standard deviation of 85 days (range, -165 to 177 days).

### Patients with liver fibrosis demonstrate significant correlation of T2 to fibrosis stage

Pathologic evaluation of all human data from biopsies, demonstrated no evidence of increased lipids or iron

deposition to suggest any contamination of our T2 relaxometry results with concomitant hemochromatosis or steatosis. Examples of ROI (yellow ellipse—*Figure 1A,B*) from T2 weighted MRI (TE =60,120; TR =2,000) within the right lobe of the liver of patients with chronic hepatitis C, avoiding major vessels avoiding areas suffering from phase encoding artifact. There was a monotonically increasing mean T2 value with increasing degree of fibrosis (*Figure 1C,D*) [control 65.4±2.9 ms (n=6); mild (Ishak 1–2) 66.7±1.9 ms (n=30); moderate (Ishak 3–4) 71.6±1.7 ms (n=26); severe (Ishak 5–6) 72.4±1.4 ms (n=61)], with relatively low standard error (~2.9 ms). There was a

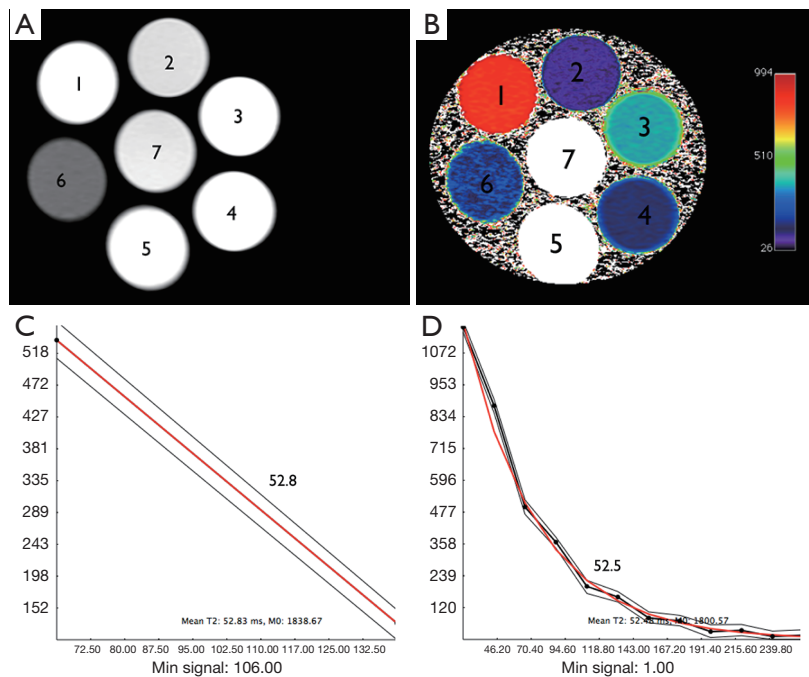


**Figure 2** T2 measures in a phantom containing multiple different T2 values. (A) T2 weighted (TE =8/TR =2,000) axial image of a phantom which consisted of one cc of dextran coated magnetic iron oxide nanoparticle (MION 48) ( $R_2=49\text{ s}^{-1}$ ) (1 mg Fe/mL) diluted with the following fractionations (1:50, 1:100, 1:250, 1:500, 1:1,000, 1:10,000, normal saline) and placed in 50 cc Eppendorf (Fischer Scientific) tubes. Note the decreased signal intensity with increased iron oxide concentration within our phantom (seven Eppendorf tubes, with serial dilutions of MNP ranging from 1:50–1:10,000). The numbers overlaid on the phantom indicate level of dilution within that specific tube. T2 was quantified using a dual echo TSE sequence (C) and compared with a CPMG sequence (D) that used two equivalent echo times to that of the TSE, and next serial increases in number of echoes from 4 to 16 echoes. The range of echo times was preserved. T2 was then quantified by using a mono-exponential fit with a customized plug-in for Macintosh based DICOM viewer and image analysis platform (Osirix®). The tubes that demonstrated T2 values that were out of range (e.g., T2 <10, and T2 >300) of human physiology were not included in this analysis. The results from tubes 2, 3 and 4 are tabulated (Table 1) and a pseudocolored map of T2 is shown (B). Paired *t*-test comparing T2 from both methods demonstrated no statistically significant difference between the approaches.

statistically significant difference between degrees of mild *vs.* severe fibrosis ( $P=0.03$ ) as determined by logistic regression dichotomizing the data between Ishak grades of <4 *vs.* Ishak >4. These results approached statistical significance ( $P<0.07$ ) when using liver function tests as covariates. Expanding on these results with ordinal logistic regression demonstrated statistical significance comparing T2 to Ishak subgroup alone ( $P=0.01$ ) and using inflammation as a covariate ( $P=0.03$ ). These results approached statistical significance amongst all groups by ANOVA ( $P=0.07$ ). Furthermore, there was no correlation between AST *vs.* T2 ( $R^2=0.00004$ ) and ALT *vs.* T2 ( $R^2=0.00007$ ) (Figure 1E,F).

#### *Dual echo TSE demonstrates equivalent T2 as that obtained from multi-echo CPMG*

The signal intensity of the phantom tubes (seven Eppendorf tubes, with serial dilutions of MNP ranging from 1:50–1:10,000) from the T2 weighted MRI (TE =8 ms/TR =2,000 ms) demonstrate no evidence of shading or dependent settling of the iron oxide nanoparticles (Figure 2A). The pseudocolored T2 maps demonstrate appropriate variation in T2 with level of dilution (Figure 2B). Examples of fits from mono-exponential fits from multiecho T2 data (Figure 2C) and 2 echo TSE (Figure 2D), are shown. The numbers overlaid on the phantom indicate level of dilution

**Table 1** T2 (ms) measured in select phantoms comparing CPMG and TSE

Number of echoes	Tube 2 (1:250)	Tube 3 (1:500)	Tube 4 (1:1,000)
16 echoes CPMG	63±4	102±2	191±2
12 echoes CPMG	52±3	102±2	192±2
8 echoes CPMG	52±5	103±1	194±2
4 echoes CPMG	54±1	110±2	218±7
2 echoes CPMG	56±3	116±3	242±10
2 echoes TSE	53±2	103±2	188±6

within that specific tube. The tubes that demonstrated T2 values that were out of range (e.g., T2 <10, and T2 >300) of human physiology were not included in this analysis. The results from tubes 2, 3 and 4 are tabulated (Table 1). Table 1 shows the values obtained from all sequences utilized. The values in Table 1 demonstrate that the TSE dual echo values are virtually identical to the 12 and in most cases 16 echo CPMG sequence results for the phantoms with T2 values most relevant to that obtained in human liver. Statistical analyses (paired *t*-test) demonstrates no evidence of statistically significant difference between any of the results (P=0.9).

#### ***DEN rat model of liver fibrosis demonstrates significant correlation of T2 to fibrosis stage***

There was homogeneous and lower signal intensity in the normal PBS control rat (Figure 3A) as compared to the heterogeneous and hyperintense signal intensity on T2 weighted imaging in the rat with advanced cirrhosis [Figures 3B (DEN 5-week) and 3C (DEN 8-week)]. Histologic analysis included H&E (Figure 3D-F) and Masson's Trichrome stains (Figure 3G-I) and are demonstrated at a magnification of 100×. On H&E stains, normal rats (Figure 3D) demonstrated decreased distortion of the normal hepatic architecture with periportal bridging (Figure 3E,F), and increased septal bands of collagen as noted on trichrome stains (Figure 3H,I) in the fibrotic and cirrhotic rats without evidence of hemochromatosis or fatty infiltration within the liver. Pathologic classification of these histologic slices demonstrated that all PBS animals demonstrated normal architecture, DEN 5 week rats corresponded to Ishak stage 3–4 fibrosis, and DEN 8-week rats, corresponded to Ishak stage 6 cirrhosis. No dysplastic nodule or hepatocellular carcinoma was evidenced at the cirrhotic (DEN 8-week) timepoint.

ROI's were placed in the right lobe of the liver in an area

of the liver excluding major vessels (Figure 4A,B) and areas with phase encoding respiratory artifact (yellow elliptical ROI, Figure 3A,B) in the normal PBS rat (Figure 4A), and cirrhotic (DEN 8) rat (Figure 4B). Quantitative relaxometry demonstrated excellent quality of fit (Figure 4C).

Quantitative analysis of T2 in each of these subgroups demonstrated an increase in the T2 between each rat subgroup [(PBS (25.2±0.8) ms, DEN 5-week (31.1±1.5) ms, and DEN 8-week (49.4±0.4) ms]. Furthermore, there was a statistically significant difference between all groups (ANOVA P<0.0001) (Figure 4D,E).

## **Discussion**

Hepatic fibrosis is the final common pathway for patients with chronic liver insults and is now known to be a dynamic process that may be partially or wholly reversible. Chronic liver damage involves hepatocyte necrosis and apoptosis (31). In response to the inflammatory mediators released in response to damage, activation of innate immunity may take place early in the insult (31). There may be a close topographical relationship between inflamed areas of the liver and those areas that develop fibrosis (20,28,41). The presence of these inflammatory cells could be a source of increased T2 value (20,28,41). The purpose of this study was to demonstrate that there was in fact a difference in T2 as quantified by MRI that correlated with severity of fibrosis.

It has been long observed by radiologists that the cirrhotic liver is "brighter" on T2 weighted images (26). Preliminary quantitative analysis in animals (20) and humans (29) has suggested that T2 may be able serve as an imaging biomarker of liver fibrosis. This is the first report to demonstrate in humans with verification in animals that varying grades of fibrosis hold statistically significant differences in T2, and therefore places a value to this long-held observation (20,28,41). Our retrospective analysis demonstrates that there is a monotonically increasing T2

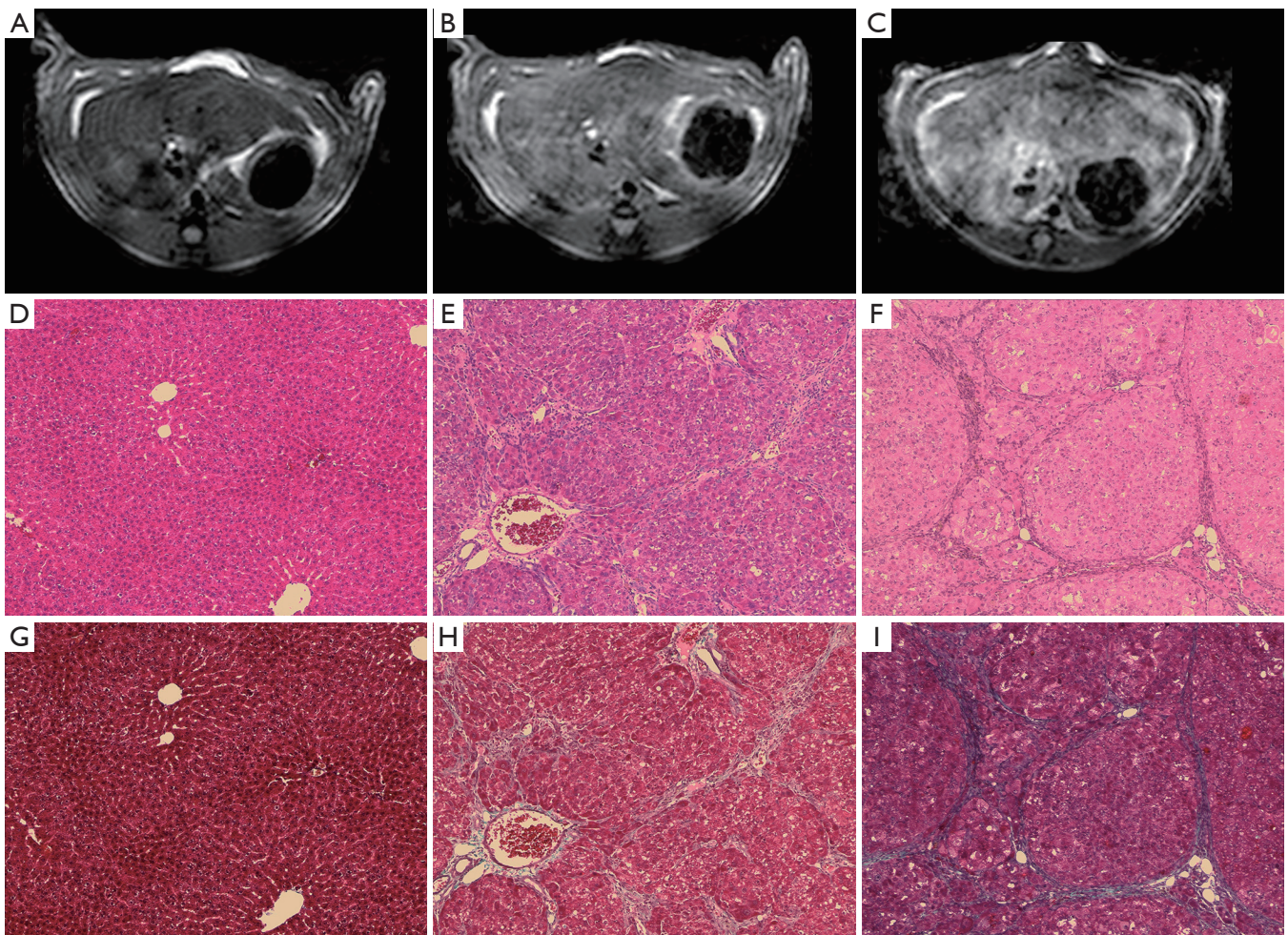


**Figure 3** DEN model of liver fibrosis comparing T2 weighted imaging with histopathology (A-C) T2 weighed MR images (TE =30/TR =2,000) of rats with varying degrees of liver fibrosis [(A) PBS control, (B) DEN 5-week, (C) DEN 8-week]. Note the heterogeneous and hyperintense signal intensity in the rat with advanced cirrhosis as compared to more homogeneous and lower signal intensity in the normal PBS control rat. Histologic analysis included hematoxylin and eosin (H&E) (D-F) and Masson's Trichrome stains (G-I) and are demonstrated at a magnification of 100 $\times$ . On H&E stains, please note the increased distortion of the normal hepatic architecture with periportal bridging, and increased septal bands of collagen as noted on trichrome stains. Pathologic classification of these histologic slices demonstrated that all PBS animals demonstrated normal architecture, DEN 5-week rats corresponded to Ishak stage 3–4 fibrosis, and DEN 8-week rats, corresponded to Ishak stage 6 cirrhosis. PBS, phosphate buffer solution; DEN, diethylnitrosamine.

value with increasing fibrosis stage, as has been noted in other imaging methods, most notable [MR elastography (42), and DWI (43)]. Although some recent results do not demonstrate a quantitative relationship between T2 and liver fibrosis stage (21,24,41), other results in animal models of liver fibrosis and in humans with chronic liver disease, suggest that the T2 value has the potential to separate varying degrees of liver fibrosis in rodent models of liver fibrosis (20,25,28,29). The values obtained in humans and rats in this study corroborate numerically values found

in the literature (20–22,28,41,44). Although the basis for this finding is unknown, it may be related to an increased inflammatory component that has been demonstrated in chronic hepatitis (30) and steatohepatitis (31). The finding that there is an association of liver fibrosis with T2 using serum biomarkers of liver inflammation as covariates may support this as well. While it is acknowledged that the sensitivity of MRE is significantly greater than MRI, the data presented here demonstrate similar sensitivity to that shown with DWI (43).

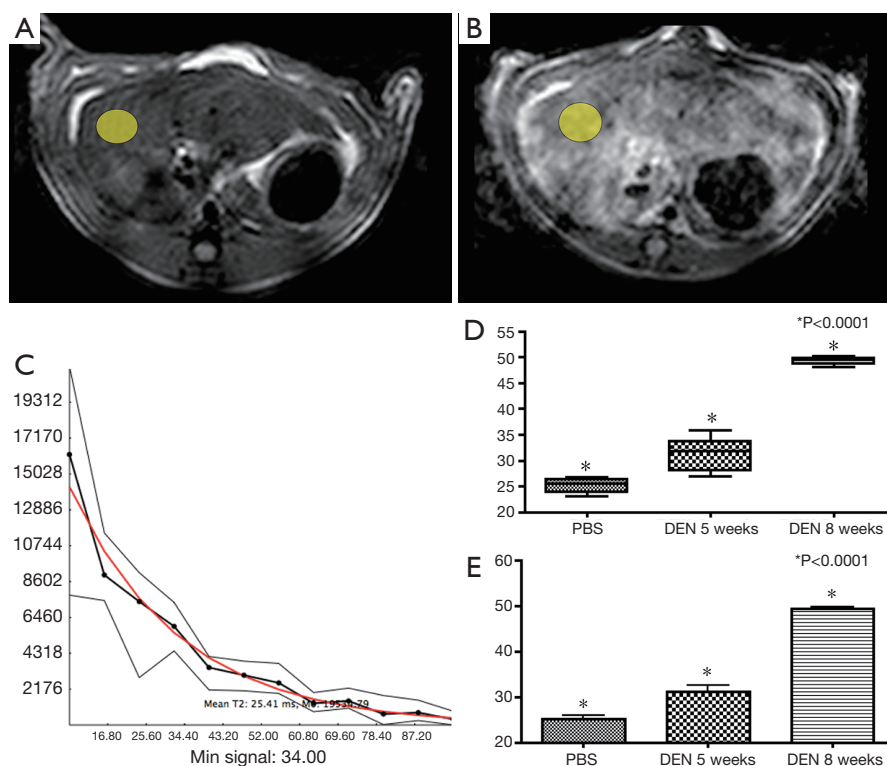


**Figure 4** Quantitative analysis of T2 data from DEN rat model of liver fibrosis compared to ISHAK staging. T2 weighted (TE =17.2 ms/TR =2,000) of a normal PBS rat (A), and cirrhotic (DEN 8) rat (B), depicting the placement of ROI, which were placed within the right lobe in an area of the liver excluding major vessels and areas with phase encoding respiratory artifact (yellow elliptical ROI). (C) Quality of the T2 fit from the measures obtained in the PBS control rat liver obtained from customized software using the Osirix platform (Osirix®). (D) Box and whisker plots, and vertical column bar graphs (E) performed for each rat subgroup (n=4 PBS normal control rats; n=5 DEN rats treated for 5 weeks, corresponding to moderate (Ishak stage 4) fibrosis; and n=4 DEN rats treated for 8 weeks, which corresponded histologically to Ishak stage 6 cirrhosis). T2 in each of these subgroups demonstrated a monotonic increase in T2 between each rat subgroup [(PBS (25.2±0.8) ms, DEN 5-week (31.1±1.5) ms, and DEN 8-week (49.4±0.4) ms], which confirmed our hypothesis and observation of increased T2 signal with liver fibrosis. Furthermore, there was a statistically significant difference between all groups (ANOVA P<0.0001) (\*). PBS, phosphate buffer solution; DEN, diethylnitrosamine.

One potential limitation of this retrospective analysis is the large variance and difficulty in quantifying T2 with only two values, and consequently, a lower statistical certainty associated with the fitting algorithms performed. Our phantom data demonstrate, however, close agreement in absolute T2 values when comparing a 2 point fit from TSE/TSE data as compared to conventional T2 quantification with multi-echo CPMG data in T2 values that are relevant for the liver. The large variance noted in the patient data may reflect inherent variance in the disease process and inflammatory infiltrate, or that the mean value agrees with the mean value from CPMG, but adds increased variance in the measure. In addition, there is increasing interest in quantitative MR imaging based

biomarkers associated with liver fibrosis (15,41). Of these, T2 relaxometry is relatively B0 and B1 insensitive and reproducible (45), relative to other relaxometry techniques that have also have been shown to be sensitive to liver fibrosis (20,28,41,45).

Our animal data also demonstrate an increasing T2 value with increasing stage of liver fibrosis. The choice of the DEN model could be criticized as it is not an established model of liver fibrosis, but it does progress through varying histologically identical phases of liver fibrosis prior to eventual HCC, a pattern that closely mimics hepatitis C and is the most relevant in the patient population studied. This sequential progression of liver fibrosis is not found in many animal models. Traditionally, DEN is administered once at

a very high-dose at a young age when hepatocytes are still proliferating as an “initiation” event (46). Phenobarbital or thioacetamide are then given as “promotion”. In this traditional initiation/promotion model, the DEN damaged hepatocytes will turn into HCCs months later in an otherwise normal liver (46). We gave DEN repeatedly at a low-dose with no promotion. In this model, HCCs arise from dysplastic nodules in cirrhotic livers—thus our model more closely represents human disease (33,47). Detailed histologic examination of these rats at this time-point did not demonstrate any evidence of HCC.

The DEN-treated rats were an excellent model of chronic liver disease and the 1 week wash-out period chosen allowed for amelioration of the acute inflammation associated with the genotoxic agents. Although our model did not have examples of each of the six Ishak stages of liver fibrosis, the histologic scoring of the PBS rats corresponded to a fibrosis stage of 0, and the rats treated with 4 weeks of DEN corresponded to a liver fibrosis stage of 3–4, and lastly those rats treated with 8 weeks of DEN, corresponded to a liver fibrosis stage of 6. Applying statistical tests to the T2 data, demonstrated statistically significant differences amongst all groups tested ( $P < 0.001$ ), with small variance. The reduced variance in these data may represent a more homogeneous liver fibrosis, or perhaps, a decreased variance with a 16 point fit of the T2.

In summary, our results corroborate the existence of a MRI-quantifiable difference that can be measured in patients with varying degrees of liver fibrosis. The T2 relaxation parameter can be quantified using a simple dual echo turbo-spin echo technique, and can potentially separate patients with mild from patients with severe liver fibrosis, which implies that T2 may be a contributory measure amongst other imaging biomarkers of liver fibrosis. We propose that this study warrants further examination of this biomarker in a prospective trial comparing T2 to other more established, robust surrogate markers of fibrosis, or as part of a multiparametric approach to the study of liver fibrosis in humans.

### Acknowledgements

None.

### Footnote

*Conflicts of Interest:* The authors have no conflicts of interest to declare.

### References

1. Bell BP, Manos MM, Zaman A, Terrault N, Thomas A, Navarro VJ, Dhotre KB, Murphy RC, Van Ness GR, Stabach N, Robert ME, Bower WA, Bialek SR, Sofair AN. The epidemiology of newly diagnosed chronic liver disease in gastroenterology practices in the United States: results from population-based surveillance. *Am J Gastroenterol* 2008;103:2727-36; quiz 2737.
2. Vong S, Bell BP. Chronic liver disease mortality in the United States, 1990-1998. *Hepatology* 2004;39:476-83.
3. Ahmed A, Keeffe EB. Hepatitis C virus and liver transplantation. *Clin Liver Dis* 2001;5:1073-90.
4. Kim WR, Brown RS Jr, Terrault NA, El-Serag H. Burden of liver disease in the United States: summary of a workshop. *Hepatology* 2002;36:227-42.
5. Talwalkar JA, Yin M, Fidler JL, Sanderson SO, Kamath PS, Ehman RL. Magnetic resonance imaging of hepatic fibrosis: emerging clinical applications. *Hepatology* 2008;47:332-42.
6. Manning DS, Afdhal NH. Diagnosis and quantitation of fibrosis. *Gastroenterology* 2008;134:1670-81.
7. Lewin M, Poujol-Robert A, Boëlle PY, et al. Diffusion-weighted magnetic resonance imaging for the assessment of fibrosis in chronic hepatitis C. *Hepatology* 2007;46:658-65.
8. Guha IN, Rosenberg WM. Noninvasive assessment of liver fibrosis: serum markers, imaging, and other modalities. *Clin Liver Dis* 2008;12:883-900, x.
9. Wai CT, Greenon JK, Fontana RJ, Kalbfleisch JD, Marrero JA, Conjeevaram HS, Lok AS. A simple noninvasive index can predict both significant fibrosis and cirrhosis in patients with chronic hepatitis C. *Hepatology* 2003;38:518-26.
10. Shaheen AA, Wan AF, Myers RP. FibroTest and FibroScan for the prediction of hepatitis C-related fibrosis: a systematic review of diagnostic test accuracy. *Am J Gastroenterol* 2007;102:2589-600.
11. Castera L. Transient elastography and other noninvasive tests to assess hepatic fibrosis in patients with viral hepatitis. *J Viral Hepat* 2009;16:300-14.
12. Del Poggio P, Colombo S. Is transient elastography a useful tool for screening liver disease? *World J Gastroenterol* 2009;15:1409-14.
13. Friedrich-Rust M, Zeuzem S. Reproducibility and limitations of transient elastography. *Liver Int* 2009;29:619-20.
14. Lucidarme D, Foucher J, Le Bail B, Vergniol J, Castera

- L, Duburque C, Forzy G, Filoche B, Couzigou P, de Lédighen V. Factors of accuracy of transient elastography (fibroscan) for the diagnosis of liver fibrosis in chronic hepatitis C. *Hepatology* 2009;49:1083-9.
15. Bonekamp S, Kamel I, Solga S, Clark J. Can imaging modalities diagnose and stage hepatic fibrosis and cirrhosis accurately? *J Hepatol* 2009;50:17-35.
  16. Huwart L, Sempoux C, Vicaud E, Salameh N, Annet L, Danse E, Peeters F, ter Beek LC, Rahier J, Sinkus R, Horsmans Y, Van Beers BE. Magnetic resonance elastography for the noninvasive staging of liver fibrosis. *Gastroenterology* 2008;135:32-40.
  17. Mariappan YK, Rossman PJ, Glaser KJ, Manduca A, Ehman RL. Magnetic resonance elastography with a phased-array acoustic driver system. *Magn Reson Med* 2009;61:678-85.
  18. Yin M, Talwalkar JA, Glaser KJ, Manduca A, Grimm RC, Rossman PJ, Fidler JL, Ehman RL. Assessment of hepatic fibrosis with magnetic resonance elastography. *Clin Gastroenterol Hepatol* 2007;5:1207-1213.e2.
  19. Taouli B, Tolia AJ, Losada M, Babb JS, Chan ES, Bannan MA, Tobias H. Diffusion-weighted MRI for quantification of liver fibrosis: preliminary experience. *AJR Am J Roentgenol* 2007;189:799-806.
  20. Aubé C, Moal F, Oberti F, Roux J, Croquet V, Gallois Y, Argaud C, Caron C, Calès P. Diagnosis and measurement of liver fibrosis by MRI in bile duct ligated rats. *Dig Dis Sci* 2007;52:2601-9.
  21. Heye T, Yang SR, Bock M, Brost S, Weigand K, Longerich T, Kauczor HU, Hosch W. MR relaxometry of the liver: significant elevation of T1 relaxation time in patients with liver cirrhosis. *Eur Radiol* 2012;22:1224-32.
  22. Hoad CL, Palaniyappan N, Kaye P, Chernova Y, James MW, Costigan C, Austin A, Marciani L, Gowland PA, Guha IN, Francis ST, Aithal GP. A study of T<sub>1</sub> relaxation time as a measure of liver fibrosis and the influence of confounding histological factors. *NMR Biomed* 2015;28:706-14.
  23. Wang YX, Yuan J, Chu ES, Go MY, Huang H, Ahuja AT, Sung JJ, Yu J. T1rho MR imaging is sensitive to evaluate liver fibrosis: an experimental study in a rat biliary duct ligation model. *Radiology* 2011;259:712-9.
  24. Lee MJ, Kim MJ, Yoon CS, Han SJ, Park YN. Evaluation of liver fibrosis with T2 relaxation time in infants with cholestasis: comparison with normal controls. *Pediatr Radiol* 2011;41:350-4.
  25. Kreft B, Dombrowski F, Block W, Bachmann R, Pfeifer U, Schild H. Evaluation of different models of experimentally induced liver cirrhosis for MRI research with correlation to histopathologic findings. *Invest Radiol* 1999;34:360-6.
  26. Ohno A, Ohta Y, Ohtomo K, Hirata K, Takatsuki K, Mochida S, Ogata I, Itai Y, Iio M, Fujiwara K. Magnetic resonance imaging in chronic liver disease evaluated in relation to hepatic fibrosis--clinical and experimental results. *Radiat Med* 1990;8:159-63.
  27. Kita K, Kita M, Sato M, Ooshima A, Yamada R. MR imaging of liver cirrhosis. *Acta Radiol* 1996;37:198-203.
  28. Guimaraes AR, Siqueira L, Boland G, Gervais D, Chew M, Hahn P. T2 relaxation time as a surrogate marker of liver fibrosis. *Proc Intl Soc Mag Reson Med* 2011;1:395.
  29. Siqueira L, Chew M, Hahn PF, Boland G, White LT, Gervais D, Mueller PR, Guimaraes AR. T2 relaxation time as a surrogate marker of liver fibrosis. *Proc Intl Soc Mag Reson Med* 2010;18:259.
  30. Oo YH, Shetty S, Adams DH. The role of chemokines in the recruitment of lymphocytes to the liver. *Dig Dis* 2010;28:31-44.
  31. Anstee QM, Concas D, Kudo H, Levene A, Pollard J, Charlton P, Thomas HC, Thursz MR, Goldin RD. Impact of pan-caspase inhibition in animal models of established steatosis and non-alcoholic steatohepatitis. *J Hepatol* 2010;53:542-50.
  32. Huang KW, Huang YC, Tai KF, Chen BH, Lee PH, Hwang LH. Dual therapeutic effects of interferon-alpha gene therapy in a rat hepatocellular carcinoma model with liver cirrhosis. *Mol Ther* 2008;16:1681-7.
  33. Schiffer E, Housset C, Cacheux W, Wendum D, Desbois-Mouthon C, Rey C, Clergue F, Poupon R, Barbu V, Rosmorduc O. Gefitinib, an EGFR inhibitor, prevents hepatocellular carcinoma development in the rat liver with cirrhosis. *Hepatology* 2005;41:307-14.
  34. Hoshida Y, Fuchs BC, Tanabe KK. Prevention of hepatocellular carcinoma: potential targets, experimental models, and clinical challenges. *Curr Cancer Drug Targets* 2012;12:1129-59.
  35. Fuchs BC, Hoshida Y, Fujii T, Wei L, Yamada S, Lauwers GY, McGinn CM, DePeralta DK, Chen X, Kuroda T, Lanuti M, Schmitt AD, Gupta S, Crenshaw A, Onofrio R, Taylor B, Winckler W, Bardeesy N, Caravan P, Golub TR, Tanabe KK. Epidermal growth factor receptor inhibition attenuates liver fibrosis and development of hepatocellular carcinoma. *Hepatology* 2014;59:1577-90.
  36. Hahn PF, Gervais DA, O'Neill MJ, Mueller PR. Nonvascular interventional procedures: analysis of a 10-year database containing more than 21,000 cases. *Radiology* 2001;220:730-6.

37. Hahn PF, Guimaraes AR, Arellano RS, Mueller PR, Gervais DA. Nonvascular interventional procedures in an urban general hospital: analysis of 2001-2010 with comparison to the previous decade. *Acad Radiol* 2015;22:904-8.
38. Team RC. R: a language and environment for statistical computing, 2013. Available online: <https://www.r-project.org/about.html>
39. Venables WN, Ripley BD. *Modern applied statistics with S*. 4 edition. Philadelphia: Springer, 2011.
40. Hawkins P, Morton DB, Burman O, Dennison N, Honess P, Jennings M, Lane S, Middleton V, Roughan JV, Wells S, Westwood K; UK Joint Working Group on Refinement BVAWF/FRAME/RSPCA/UFAW. A guide to defining and implementing protocols for the welfare assessment of laboratory animals: eleventh report of the BVAWF/FRAME/RSPCA/UFAW Joint Working Group on Refinement. *Lab Anim* 2011;45:1-13.
41. Cassinotto C, Feldis M, Vergniol J, Mouries A, Cochet H, Lapuyade B, Hocquelet A, Juanola E, Foucher J, Laurent F, De Ledinghen V. MR relaxometry in chronic liver diseases: comparison of T1 mapping, T2 mapping, and diffusion-weighted imaging for assessing cirrhosis diagnosis and severity. *Eur J Radiol* 2015;84:1459-65.
42. Huwart L, Sempoux C, Salameh N, Jamart J, Annet L, Sinkus R, Peeters F, ter Beek LC, Horsmans Y, Van Beers BE. Liver fibrosis: noninvasive assessment with MR elastography versus aspartate aminotransferase-to-platelet ratio index. *Radiology* 2007;245:458-66.
43. Do RK, Chandarana H, Felker E, Hajdu CH, Babb JS, Kim D, Taouli B. Diagnosis of liver fibrosis and cirrhosis with diffusion-weighted imaging: value of normalized apparent diffusion coefficient using the spleen as reference organ. *AJR Am J Roentgenol* 2010;195:671-6.
44. Chow AM, Gao DS, Fan SJ, Qiao Z, Lee FY, Yang J, Man K, Wu EX. Measurement of liver T<sub>1</sub> and T<sub>2</sub> relaxation times in an experimental mouse model of liver fibrosis. *J Magn Reson Imaging* 2012;36:152-8.
45. Wood JC, Zhang P, Rienhoff H, Abi-Saab W, Neufeld EJ. Liver MRI is more precise than liver biopsy for assessing total body iron balance: a comparison of MRI relaxometry with simulated liver biopsy results. *Magn Reson Imaging* 2015;33:761-7.
46. Huang X, Yu C, Jin C, Yang C, Xie R, Cao D, Wang F, McKeehan WL. Forced expression of hepatocyte-specific fibroblast growth factor 21 delays initiation of chemically induced hepatocarcinogenesis. *Mol Carcinog* 2006;45:934-42.
47. Corpechot C, Barbu V, Wendum D, Kinnman N, Rey C, Poupon R, Housset C, Rosmorduc O. Hypoxia-induced VEGF and collagen I expressions are associated with angiogenesis and fibrogenesis in experimental cirrhosis. *Hepatology* 2002;35:1010-21.

**Cite this article as:** Guimaraes AR, Siqueira L, Uppal R, Alford J, Fuchs BC, Yamada S, Tanabe K, Chung RT, Lauwers G, Chew ML, Boland GW, Sahani DV, Vangel M, Hahn PF, Caravan P. T2 relaxation time is related to liver fibrosis severity. *Quant Imaging Med Surg* 2016;6(2):103-114. doi: 10.21037/qims.2016.03.02